PERGAMON

International Journal of Solids and Structures 38 (2001) 1919–1933

INTERNATIONAL JOURNAL OF SOLIDS and STRUCTURES

www.elsevier.com/locate/ijsolstr

Nonlinear vibrations in the apex of guinea-pig cochlea

S.M. Khanna [a,*], L.F. Hao [b]

[a] *Department of Otolaryngology and Head and Neck Surgery, College of Physicians and Surgeons of Columbia University, 630 West 168th Street, New York, NY 10032, USA*

[b] *Department of Otolaryngology and Head and Neck Surgery, University of Maryland School of Medicine, Baltimore, MD 21201, USA*

Received 6 September 1999; in revised form 18 December 1999

Abstract

The apical turn of a living guinea-pig cochlea was opened gently and fluid coupled to the objective lens of a confocal microscope-interferometer. The reticular lamina was viewed through the intact Reissner's membrane. Mechanical vibrations were measured at identified cellular locations, in response to tones applied with an acoustic transducer coupled to the ear canal. Time waveforms were measured at an outer and middle Hensen's cell over a wide intensity and frequency range. The time waveforms were distorted and the magnitude and number of harmonics in the FFTs of waveforms were high, indicating a strong nonlinearity. However, the amplitude of the fundamental component of the response increased nearly linearly with sound pressure. This paper examines the origin and the role of the nonlinear components in the cochlear function.

Keywords: Guinea Pig; Cochlea; Hensen's cell; Mechanical vibrations; Micromechanics; Nonlinear waveforms; FFT

1. Introduction

The organ of hearing consists of the external ear, middle ear and the inner ear. The acoustical signals collected by the external ear act on the middle ear, driving the stapes to produce fluid motion in cochlea (Wever and Lawrence, 1954). The cochlea is a coiled structure, shaped like a snail shell, with three fluid filled canals: scala vestibuli (SV), scala media (SM) and scala tympani (ST). The middle canal (SM) is triangular in shape and contains the hearing organ (Fig. 1). The basilar membrane (BM) forms the base of the SM and Reissner's membrane, the dividing partition between the SV and SM.

Fluid motion in the canals is coupled to the BM and causes it to vibrate (Békésy, 1960). Extensive literature on the modeling of fluid and BM motion is available (Zwislocki, 1948; Steele, 1974; de Boer, 1984).

The cochlea is tuned. The base is tuned to high frequencies and the apex to low frequencies. The frequency map of the cochlea is arranged from high to low frequencies from the base to the apex. It was

* Corresponding author. Tel.: +1-212-305-3993; fax: +1-212-305-4045.
E-mail address: smk3@columbia.edu (S.M. Khanna).

0020-7683/01/$ - see front matter
PII: S0020-7683(00)00143-8

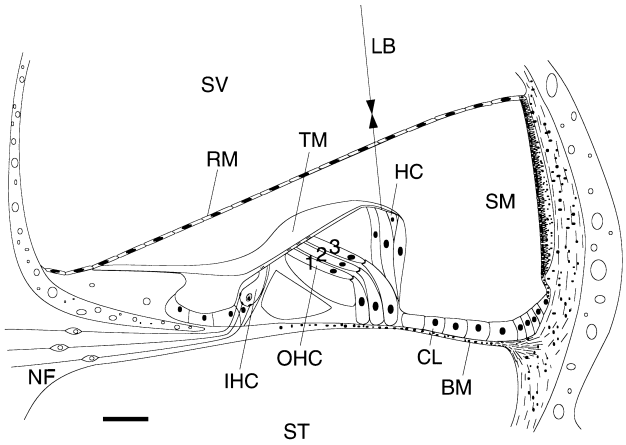

Fig. 1. Cross-section of the apical turn of the guinea-pig cochlea showing the arrangement of some of the key structures in the organ of corti. The cochlea consists of three canals: SV, SM, and ST. SV and ST are only partially shown. BM; Claudius' cells (CL); Reissner's membrane (RM); one row of IHC; three rows of OHC; and HC; RL extends from IHC to Outer HC; TM; Afferent nerve fibers (NF); Laser beam measuring HC vibration (LB).

thought that the frequency selective properties of the BM and overlying mass determined the tuning of the ear. The hearing organ was also thought to follow, passively and linearly, the BM motion (Békésy, 1960).

Some of the key features of the organ geometry are shown in Fig. 1. Deiter's cells (DC) are attached to the BM and support three rows of outer hair cells (OHC). Pillar cells (PC) and Hensen's cells (HC) provide mechanical support for the reticular lamina (RL), which extends from inner hair cells (IHC) to outer HC. The cellular organization of the organ follows the same pattern throughout the cochlea and in different mammalian ears. Functional significance of this arrangement is only poorly understood. The physical dimensions of the sensory cells and supporting structures change systematically from the base to the apex, suggesting an important role in the cochlear function (Lim, 1986; Tilney and Saunders, 1983).

Both the inner and outer hair cells have a staircase arrangement of cilia bundles at their apical end. Tips of the tallest stereocilia of the OHC are inserted into the tectorial membrane (TM). Relative motion between the RL and TM bends the stereocilia bundles and opens strain sensitive ionic channels, producing the receptor potential (Hudspeth and Corey, 1977).

The BM measurements in living animals near the basal region indicated that the response was sharply tuned and highly nonlinear. Near the frequency of maximum response, vibration amplitude increased linearly at low sound pressures but saturated at sound pressure levels above 40 dB (Rhode, 1978; Cooper, 1998; Robles et al., 1986). The tuning became broad and the vibration amplitude decreased after damage to the cochlea or death of the animal. These findings are explained by the presence of positive feedback and saturation in the basal turn (Zwicker, 1986; Cooper, 1998).

The discovery of electromotility changed the view of the OHC function from passive followers to active amplifiers and regulators. OHC change their length when an electric current is passed through them. Hyperpolarization causes the cell to elongate while depolarization results in shortening. Transcellularly applied alternating potential gradients produce symmetric displacements at low frequencies and asymmetric displacements at high frequencies. The length change was much smaller in the hyperpolarization direction as compared to depolarization (Brownell, 1983; Brownell et al., 1985).

Mechanical motility provides an alternative way in which the OHC may be excited. Alternating fluid pressure acting on the cell membrane of the OHC produces both static and alternating length changes. The

cells extracted from apical parts of the cochlea are tuned to low frequencies and those from the basal parts to high frequencies (Brundin et al., 1989; Brundin and Russell, 1994).

The mechanical signal is transduced into nerve impulses at the IHC where 95% of the afferent nerve fibers originate (Spoendlin, 1972). The detailed mechanism by which the OHC control the stimulation of the IHC is not known. However, it is clear that in transmission of the mechanical signal from the BM to the IHC, the signal undergoes sophisticated transformation and is controlled both locally and by the efferent system.

Most of the above findings were based on mechanical vibration measurements at the BM and on isolated hair cells. In order to understand the function of the hearing organ as a unit, at the cellular level, it is necessary to measure the response at different cellular locations in an intact functioning system.

Most BM vibration measurements using interferometry utilize beads (Cooper and Rhode, 1995; Gummer et al., 1996; Ruggero and Rich, 1991). The placement of beads is invasive and alters the response in the apical turn of the cochlea (Khanna et al., 1998). It is not appropriate for cellular measurements because placement of beads requires opening the structures above the cells, which produces trauma and alters the normal structure.

We developed a confocal laser heterodyne interferometer with high optical sensitivity that allows vibration measurements directly from the normal surface of the cells. The confocal arrangement accepts light reflected from the selected surface while rejecting light from surfaces above and below.

In the basal turn of the cochlea, in the region near the characteristic frequency (CF), vibration amplitude at the fundamental frequency increases nonlinearly with sound pressure level. When the physiological condition of the cochlea is bad this nonlinearity disappears (Rhode, 1978). Several investigators have established that the presence of nonlinearity at the fundamental frequency in the basal and middle turns of the cochlea is an essential sign of normal function.

When vibrations were measured in the apical turn of the cochlea, at the level of RL in the temporal bone preparation, vibration amplitude increased from the IHC to HC, but the tuning shape remained essentially the same. In guinea-pig cochlea, HC contain lipid droplets that are highly reflective. HC, therefore make a good target to study the RL vibration. The vibration velocity at the fundamental frequency was found to increase nearly linearly with sound pressure at levels below about 90 dB SPL (Khanna et al., 1989a).

Since the lack of nonlinearity at the fundamental frequency in the basal turn has been associated with cochlear damage, some auditory scientists assumed that the linear response in the apical turn indicated a damaged cochlea. Cooper and Rhode (1995) measured cellular vibrations in the apical turn in living guinea-pig cochlea; they found a nonlinear increase with SPL in the fundamental component, but only in the notch region located in the middle of the tuning curve. In a later publication, Cooper (1996) showed that the notch was an artifact created when the cochlea was not sealed. When the cochlea was properly sealed, the notch disappeared. The nonlinearity associated with the notch should also disappear.

In our experiments with the sealed apical turn of the cochlea, the mechanical response at the fundamental frequency increased linearly with SPL. However, simply because nonlinearity is not seen at the fundamental frequency does not mean the vibratory response is linear. The time waveforms of the response are asymmetrical, and there are a large number of harmonics present (Khanna et al., 1989a,b; Khanna and Hao, 1999b). This paper presents a systematic investigation of these nonlinear components in the apical turn of cochlea in living guinea pigs. The change in the magnitude of the harmonic components with the sound pressure is highly nonlinear. The fundamental component however behaves nearly linearly and therefore presents a puzzle: How can the fundamental response show linearity in the presence of extensive waveform distortion and harmonics? It was recently shown that the negative feedback is present in the apical turn (Khanna and Hao, 1998). This negative feedback makes the response linear at the fundamental frequency. The nonlinear components are however generated outside the feedback loop and therefore not affected by it.

2. Methods

Non-pigmented guinea pigs weighing 300–600 g were anaesthetized with ketamine (87 mg/kg) and xylazine (13 mg/kg). Supplemental doses (50% of the initial dose) were given every 2 h. A ventral approach was used to access the temporal bulla. A small portion of the apical bone of the left cochlea was removed, exposing approximately one-fourth to one-third of the apical turn, leaving the modiolus, stria vascularis and Reissner's membrane intact. The details of animal preparation have been described earlier (Hao and Khanna, 1996; Khanna and Hao, 1999a,b). The cochlea was coupled to the objective lens of the confocal microscope with a plastic tube filled with tissue culture medium, forming a fluid-tight seal. Measurements of tuning curves, waveforms and spectra have been carried out on more than 100 living guinea pigs to date and support the results described in this paper. The Institutional Animal Care and Use Committee (IACUC), of Health Science Division of Columbia University, approved the care and use of the animals reported in this study.

2.1. Measuring system

The cochlea was viewed with our slit confocal microscope. This is an incident light microscope, with a confocal slit arrangement, that allows only light from regions close to the focal plane to pass through the microscope and form an image. Reflections originating from surfaces above and below the focal plane are rejected. Details of the microscope and its improvements have been presented earlier (Koester, 1980, 1990; Koester et al., 1989, 1994).

A confocal heterodyne interferometer developed by us was used for vibration measurements (Willemin et al., 1988, 1989; Khanna et al., 1996). The microscope and the interferometer share the same objective lens. Their focal planes are aligned precisely so that when the microscope is focused on a structure, and the incident laser beam is placed on it, the interferometer is automatically focused and the vibration at the selected location can be measured. The spot size and the sectioning depth of the interferometer are much smaller than cell size, so that vibrations of individual cells can be measured. The optical reflectivity of the cochlear structures is extremely low (ITER 1989), and the interferometer sensitivity is designed to be close to the theoretical maximum in order to record from these structures with good signal-to-noise ratio.

The linearity of the interferometer-frequency demodulator system is very high. Distortion levels at the highest velocity measured (6×10^{-3} m/s) are at least 60 dB below the fundamental level. Therefore, we can be sure that the nonlinearity originates in the cochlea and not in the measuring system. Demodulated interferometer output is applied to the first channel of the A/D converter.

Signals are generated, and the response is measured with a 16 bit resolution DSP system using two D/A and two A/D converters (Ariel Corp). The signals are synthesized using a PC. They are applied to an acoustic transducer with low distortion (Sokolich, 1981) after passing through an anti-aliasing filter (Wavetek 752A). The acoustic transducer is coupled to the ear canal, and the sound pressure is monitored with a Sokolich probe microphone (Sokolich, 1981), positioned approximately 7 mm in front of the tympanic membrane. The probe microphone output is amplified and passed through an anti-aliasing filter (Wavetek model 716) and applied to the second channel of the A/D converter. Averaged samples of the time waveforms for both A/D channels are stored on an optical disk.

In this study, the sampling rate used was 20.16 ks/s (sampling time 49.6 μs). The cut-off frequency of the anti-aliasing filters in both channels was set to 10 kHz. Response was averaged over 25 presentations and stored in 1024 bins. Sinusoidal signals were used for measurement. To avoid transients, the signal was played out for 254 ms before averaging. Measurements were made at 59 frequencies from 20 to 5000 Hz. Total recording time at each frequency was approximately 2.6 s with 1 s interval between presentations. A complete tuning curve (59 frequencies) takes approximately 2 min. Measurements at each set of frequencies were carried out at two sound pressure levels (approximately 80 and 90 dB SPL). In some experiments,

vibrations were measured at five selected frequencies, at sound pressure levels (SPL) between 40 and 100 dB, in increments of 2 dB.

3. Observations

In Fig. 2, we see the vibration amplitude of an outer HC measured at four frequencies (98, 151, 200, and 400 Hz), between 40 and 100 dB SPL. The characteristic frequency of this cell was 256 Hz. The sound pressure was incremented in steps of 2 dB. The amplitude at the fundamental frequency increased nearly linearly with SPL above 65 dB at 98 Hz, above 40 dB at 151 and 200 Hz, and above 45 dB at 400 Hz. It is interesting to note that the line is not perfectly straight, rather, it is composed of segments with slightly different slopes. In comparison to the fundamental, the amplitudes of the second, third and fourth harmonics change quite irregularly with sound pressure level. At 200 Hz, between 40 and 70 dB SPL, the harmonic amplitude appears to oscillate in a low-high-low pattern. We cannot be sure if this effect is real, because below 10^{-10} m amplitude, at these low frequencies, the harmonic amplitudes are near the noise floor. Between 70 and 100 dB the harmonic response increases in magnitude but displays maxima and minima.

Time waveforms of velocity amplitude, measured at middle HC located next to the outer HC (Fig. 2), are shown in Fig. 3 at six frequencies between 118 and 315 Hz. For comparison, a reference sine wave is

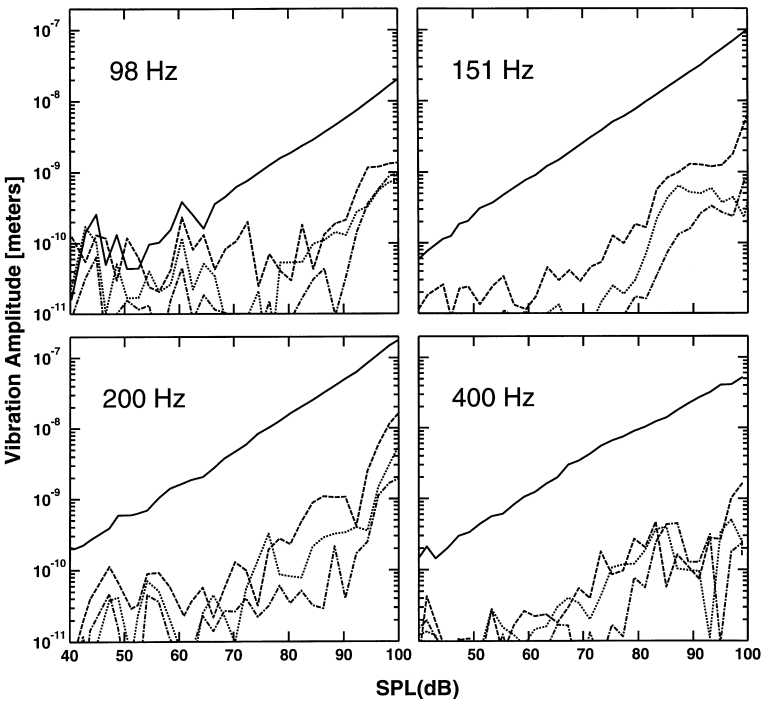

Fig. 2. Vibration amplitude of the outer HC as a function of sound pressure level at the fundamental (—), second (- - -), third (· · ·) and fourth (– · – · –) Harmonic. Data is shown at four frequencies (98, 151, 200, and 400 Hz). The characteristic frequency of the cell was 256 Hz. Vibration amplitude at the fundamental frequency increases nearly linearly with the SPL. Second, third and fourth harmonics do not show a clear pattern of behavior below 60 dB SPL. Above 70 dB SPL they increase with sound pressure; however, even in this region, the curves are quite irregular with several maxima and minima.

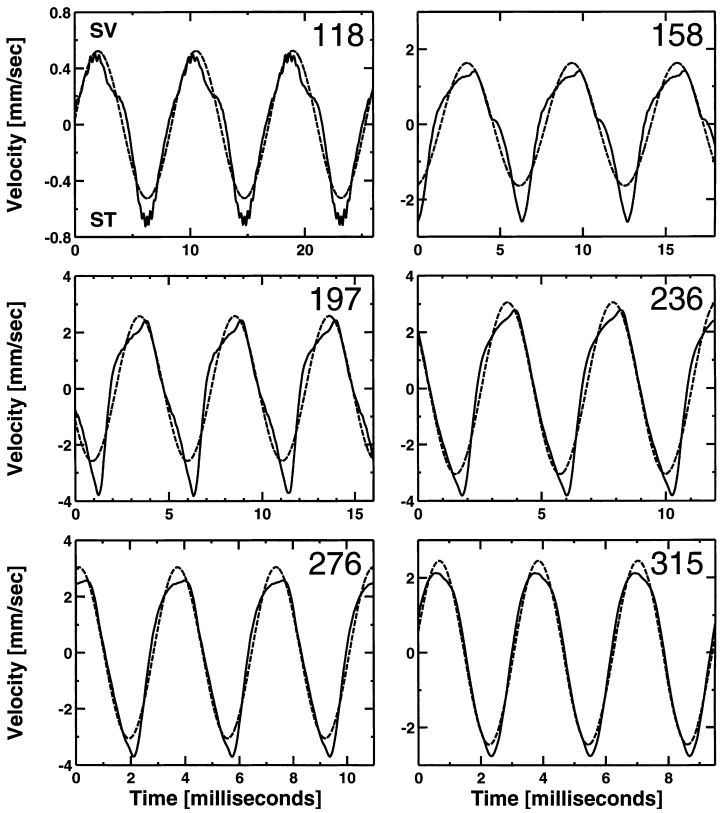

Fig. 3. Time waveforms of velocity amplitude (—) at six frequencies (118, 158, 197, 236, 276, and 315 Hz) measured at middle HC at an approximate SPL of 98 dB. For comparison, sinusoidal reference wave (···) is shown. Velocity waves are clearly distorted. Velocity is higher in the direction of ST near the CF region (118–236 Hz).

included (dotted line). The amplitude and phase of each reference sine wave is that of the fundamental component of the fast Fourier transform (FFT), shown at the corresponding frequency in Fig. 4. Compared to the reference waves, the velocity waveforms are distorted. The positive peak of the wave (towards SV) is compressed, while the negative peak (towards ST) is stretched. The nonlinearity of time waveforms decreases with SPL and is normally seen only above about 60 dB SPL.

FFTs corresponding to the time waveforms recorded at 98 dB SPL are shown Fig. 4. Spectral components at the fundamental and multiple harmonics are seen at all six frequencies. The large number of harmonics indicates that the cochlear mechanics in the apical turn are highly nonlinear.

Fig. 5 shows FFTs of the time waveforms recorded at 88 dB SPL (10 dB lower). The change in the harmonic amplitude with the harmonic number is slightly different than that seen in Fig. 4. The number of harmonics however is large, indicating a strong nonlinearity.

Tuning curves were measured at the outer HC. Vibration amplitude at the fundamental, second and third harmonics is shown in Fig. 6. The normalized vibration amplitude was obtained by integrating the velocity of the fundamental and harmonic components, then dividing it by the sound pressure at the fundamental frequency. The tuning of the harmonic curves is much sharper than that of the fundamental. The low frequency and high frequency slopes are also much steeper. This suggests that additional tuning may be present between the RL and the generation of harmonics.

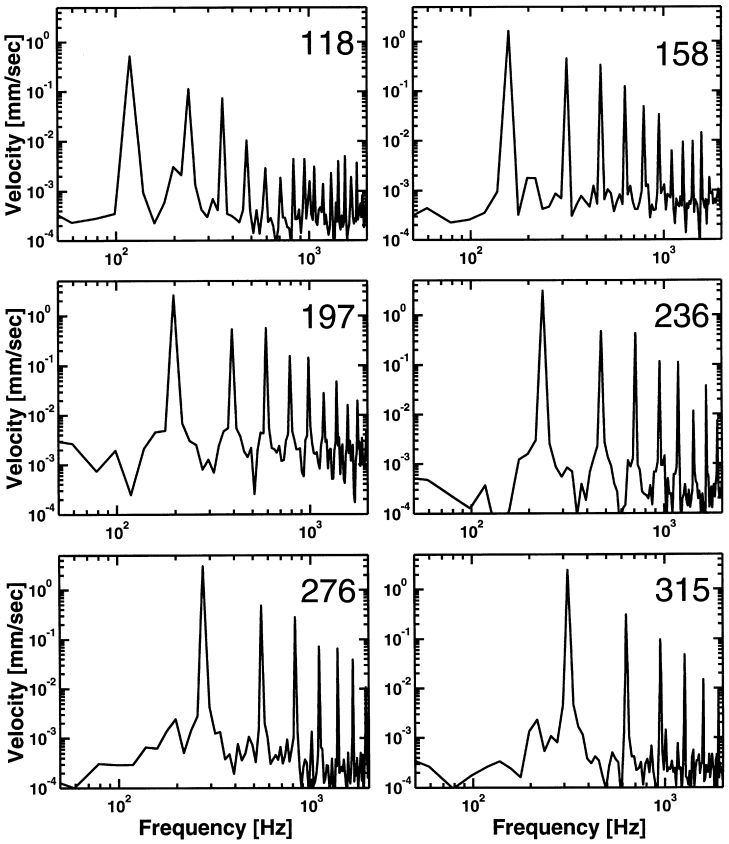

Fig. 4. FFTs of the time waveforms shown in Fig. 2. Large number of harmonics is seen at all frequencies shown. The harmonic components actually extend to a much higher frequency. The upper frequency is arbitrarily cut off in these graphs to 2.0 kHz. The harmonics basically decrease with increase in harmonic number except with a harmonic number greater than 6.

Phase characteristics for the outer HC are shown in Fig. 7. All phases are referred to the sound pressure phase. To make our data comparable to other investigators (Rhode and Cooper), who use negative sound pressure phase as the reference, 180° should be added to our phase angles. Phase curves for the fundamental, second and third harmonic can be divided into at least two segments: an initial steep slope below 500 Hz, followed by a shallower portion between 500 and 2000 Hz.

The initial slope is steeper for the harmonics as compared to the fundamental. Since the time delay is proportional to the linear part of the slope of the phase curve, the delay associated with harmonics is larger than that for the fundamental. This suggests that the harmonics are generated after the fundamental component.

Harmonic/fundamental amplitude ratios for the second and third harmonics (calculated from the data from, Fig. 5) are shown in Fig. 8. The ratio for the second harmonic is highest at low frequencies (below 20 Hz), and decreases with increasing frequency, reaching a minimum near 100 Hz. Between 100 and 400 Hz, the second and third harmonic curves show a tuning. The tuning of the third harmonic curve is sharper than that for the second harmonic. These curves represent the additional tuning associated with the nonlinear process.

Tuning sharpness of the second harmonic curves measured in 19 experiments is related to the tuning sharpness of the fundamental tuning curve in Fig. 9. Tuning sharpness is measured in

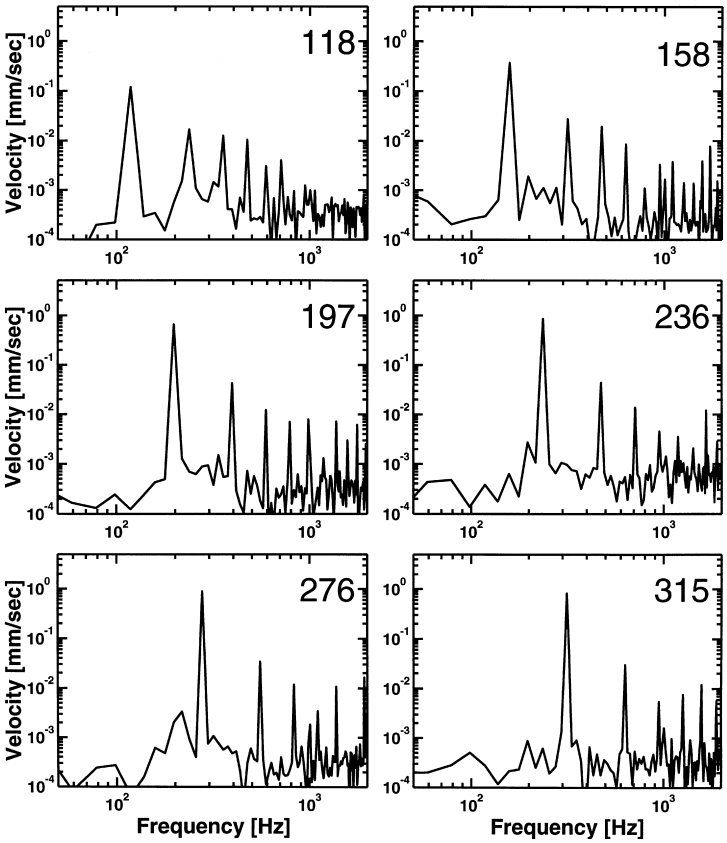

Fig. 5. FFTs of the time waveforms at the same six frequencies, and same middle HC, at an approximate SPL of 88 dB. A large number of harmonics is still visible and shows the nonlinearity of response.

$Q_{20\ \mathrm{dB}} = F_0/\mathrm{Bandwidth}$ between frequencies that are 20 dB below maximum amplitude at F_0. The sharpness of the second harmonic tuning curve is higher in cochlea with greater tuning sharpness of the fundamental. The sharpness of the fundamental tuning curve reflects the condition of the cochlea (Khanna and Hao, 1999a). Therefore, the harmonic tuning is sharper in healthier cochlea.

The maximum amplitude of the second harmonic tuning curve is plotted against the maximum amplitude of the fundamental tuning curve in Fig. 10. The second harmonic amplitude is larger in cochlea in which the fundamental amplitude is higher. The amplitude of the fundamental is related to the condition of the cochlea (Khanna and Hao, 1999a). Therefore, the second harmonic amplitude is higher in cochlea in good condition.

4. Discussion

In the apical turn of the cochlea, the vibration amplitude of the RL at the fundamental frequency increases approximately linearly with sound pressure up to about 100 dB SPL. However, the time waveforms of the vibrations at the RL, produced by sinusoidal stimulus applied to the external ear, are nonlinear. The FFTs of these time waveforms are rich in harmonics. The nonlinearity is highest at the OHC 1 (Khanna and Hao, 1999b). At the outer HC at 200 Hz, the fundamental component was above the noise floor of the

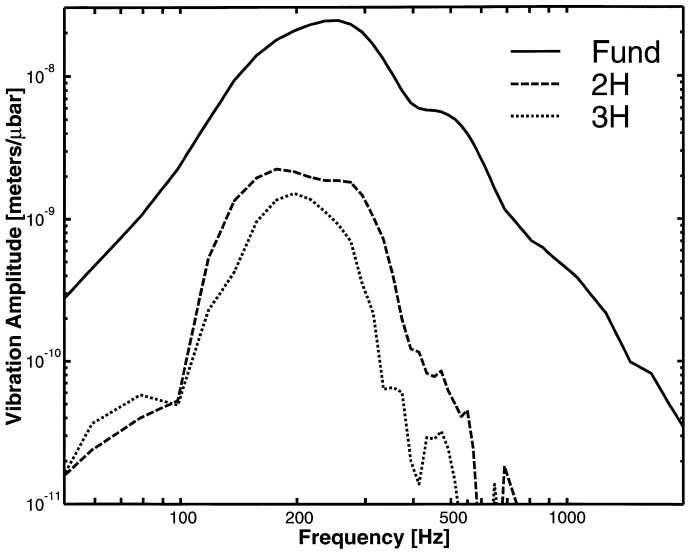

Fig. 6. Vibration amplitude of an outer HC as a function of frequency (tuning curve) at the fundamental, second, and third harmonics. The tuning of the harmonic curves is sharper as compared to the fundamental.

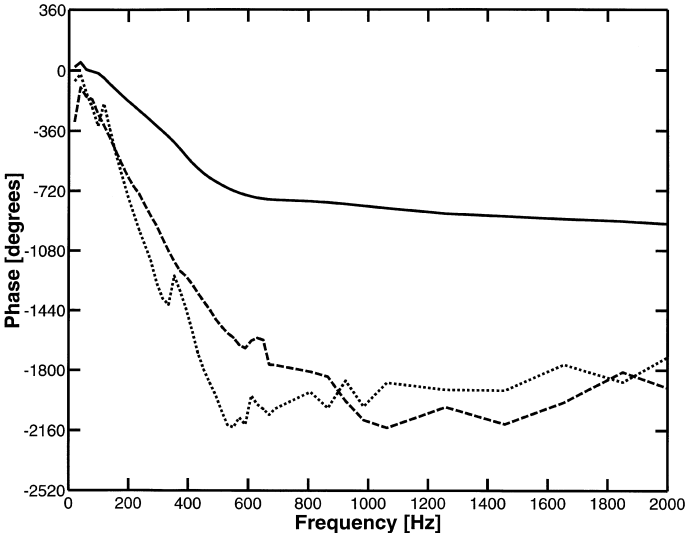

Fig. 7. Phase response of an outer HC, as a function of frequency, at the fundamental (—), second (- - -) and third harmonic (···). Phase is measured with respect to the sound pressure phase at the tympanic membrane.

FFT throughout the SPL range 40–100 dB. However, the harmonic components were seen clearly above the noise floor only above 65 dB SPL. In this region, the amplitudes of the second, third and fourth harmonics do not increase monotonically with sound pressure. The curves display numerous maxima and minima and are highly irregular. Although similar effects are also seen below 65 dB SPL, spectral amplitudes are too close to the noise floor. If we only look at the fundamental component we could be misled, concluding the response of the organ is linear, as it shows a nearly linear increase with SPL. However, looking at the time waveforms, or the FFTs of waveforms, it is clear that the response is highly *nonlinear*.

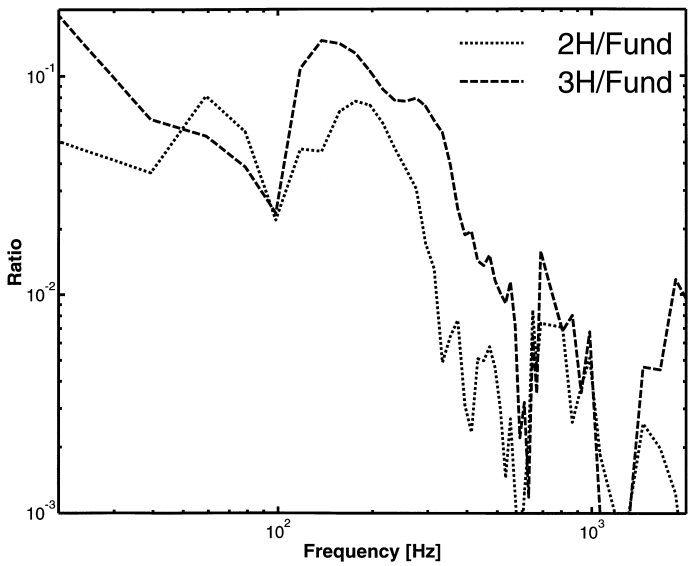

Fig. 8. Ratio of the second harmonic and the fundamental (—) and third harmonic and the fundamental (- - -). The ratio shows a tuned peak in the region 100–300 Hz.

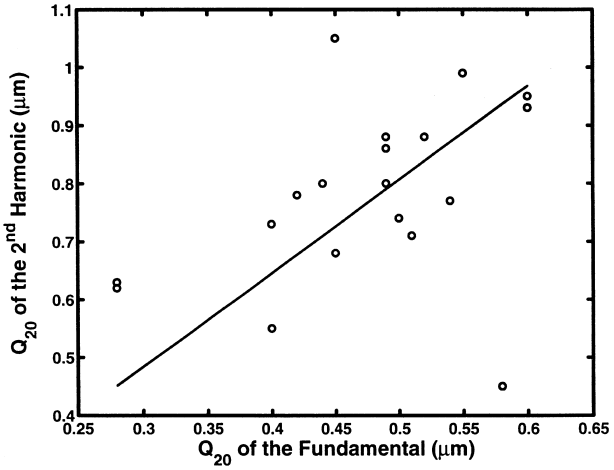

Fig. 9. $Q_{20\ \mathrm{dB}}$ of the second harmonic tuning curve plotted as a function of $Q_{20\ \mathrm{dB}}$ of the fundamental tuning curve in 19 experiments. The solid line is the least square fit to the data points. The sharpness of second harmonic tuning increases with the sharpness of tuning for the fundamental.

Cooper (1998) measured harmonic components of the BM vibration in the basal turn of the guinea pig cochlea. At 8.0 kHz (below CF), the BM amplitude at the fundamental frequency increases linearly with SPL. Second and third harmonics are seen between 55 and 100 dB SPL and increase nonlinearly with SPL. At this frequency, the SPL dependence of the fundamental and harmonics is quite similar to that observed in the apical turn. Nearer to CF however the response in the basal turn is quite different at the fundamental frequency. The difference in the response at the fundamental frequency can be explained by the presence of negative feedback in the apical turn (Khanna and Hao, 1998).

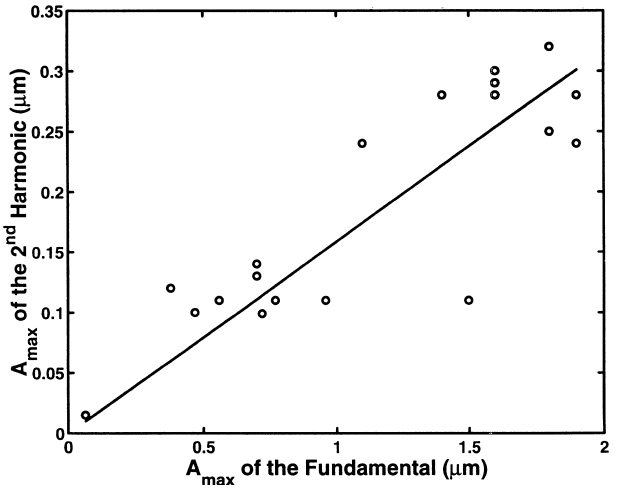

Fig. 10. Maximum amplitude of the second harmonic tuning curve plotted as a function of the maximum amplitude of the fundamental tuning curve in 19 experiments. The solid line is the least square fit to the data points. The second harmonic amplitude increases nonlinearly with the fundamental amplitude.

4.1. Analysis of the negative feedback

If V_{lf} is the RL velocity with feedback, V_{bmf}, the BM velocity with feedback, V_{bm} is the BM velocity without feedback, A_{h} is the OHC amplification and β is the fraction of the output fed back to the input, the following relations can be derived (Bode 1945; Khanna and Hao, 1998):

The RL velocity is given by

$$V_{\mathrm{lf}} = A_{\mathrm{h}} V_{\mathrm{bm}}/(1 + A_{\mathrm{h}}\beta). \tag{1}$$

When amplification is high, $A_{\mathrm{h}}\beta \gg 1$,

$$V_{\mathrm{lf}} = V_{\mathrm{bm}}/\beta. \tag{2}$$

The RL velocity is independent of the hair cell amplification A_{h}. Thus, the hair cell amplification could decrease while the vibration at the RL remains constant. However, when the gain becomes too low, the condition $A_{\mathrm{h}}\beta \gg 1$ is no longer satisfied.

When amplification is low, $A_{\mathrm{h}}\beta \ll 1$

$$V_{\mathrm{lf}} = A_{\mathrm{h}} V_{\mathrm{bm}}. \tag{3}$$

The RL velocity goes down as the hair cell amplification decreases. It is important to consider the changes taking place at the BM at the same time.

The BM velocity with feedback is given by

$$V_{\mathrm{bmf}} = V_{\mathrm{bm}}/(1 + A_{\mathrm{h}}\beta). \tag{4}$$

When amplification is high, $A_{\mathrm{h}}\beta \gg 1$

$$V_{\mathrm{bmf}} = V_{\mathrm{bm}}/A_{\mathrm{h}}\beta. \tag{5}$$

As the hair cell amplification decreases, BM velocity increases. The increase is inversely proportional to the reduction of the amplification.

When amplification becomes too low, $A_h\beta \ll 1$

$$V_{bmf} = V_{bm}. \tag{6}$$

The BM velocity does not change as the gain decreases further.

From the above analysis, the following sequence of events is predicted: When the amplification of the hair cells is reduced (i) The BM velocity increases while the RL velocity remains constant; (ii) The RL velocity decreases while the increased BM velocity remains fixed. This is exactly the sequence of events observed experimentally (Khanna and Hao, 1998). An important consequence of negative feedback is that any distortion originating in the amplification is reduced by the feedback factor $A_h\beta$ (Bode, 1945). The nonlinear components seen in the response must therefore originate outside the feedback loop.

This simple feedback model explains the basic results that were obtained experimentally, but does not predict the changes in the shape of the tuning curves that were observed at the BM and the RL. An analysis that takes these effects into account has been developed and will be the subject of a separate paper.

The amplitude of the second harmonic component increases with the amplitude of the fundamental component, and the sharpness of second harmonic tuning increases with the sharpness of the fundamental tuning curve. The amplitude at CF and the tuning sharpness of the fundamental are related to the condition of the cochlea (Khanna and Hao, 1999a). The level and sharpness of tuning of the second harmonic is high when the cochlea is in good condition. The degree of nonlinear response indicates the condition of the cochlea in both basal and the apical turns.

It is important to find out where the nonlinearity originates. Positive vibration amplitude in our measuring system indicates that the RL is moving toward the SV, and the negative amplitude indicates movement towards ST. The velocity of the RL is much higher in the direction of ST, as compared to the direction of SV. This effect is most pronounced at OHC1. This asymmetry was also seen in earlier experiments with temporal bone preparations (Khanna et al., 1989b) and in living guinea pigs (Khanna and Hao, 1999b).

The sensory hairs of both inner and outer hair cells stand perpendicular to the sensory cell surface cuticular plate and not parallel to the long axis of the sensory cell (Iurato, 1961). The angle of the hair bundle with respect to the long axis of the OHC is therefore tilted, such that the extension of the OHC would result in bending the stereocilia in the excitatory direction. In the apical turn of the cochlea, the upper surface of the (cuticular plate) OHC is in the plane of the RL. The long axis of the OHC however is tilted towards the modiolus and makes an angle of 115° with the plane of RL (ITER, 1989). The angle between the long axis of the OHC and the stereocilia bundles is about 25°. An extension of the OHC in the apical turn therefore would also result in deflection of the stereocilia outwards, in the excitatory direction.

Is the nonlinear movement of RL (Fig. 3) produced by the electromotility of the OHC? As a passive system, the RL should move in phase with BM. When the BM moves up toward the SV, the RL should follow. If the action of electromotility is taken into account, then, as the RL moves towards the SV, the stereocilia are bent in the excitatory direction, producing depolarization and contraction of OHC. This would have two effects: (i) apical end of the OHC would move down towards ST and OHC motion would subtract from the initial upward motion of the RL. (ii) The OHC base would move up towards the SV and, therefore, add to the BM motion because they move in the same direction. This would produce positive feedback increasing the BM motion.

If we sacrifice the animal, the active component producing the positive feedback should disappear, and we should see a decrease in BM motion. Instead, we experimentally observe the opposite: a large *increase* in the BM motion. This increase in the BM vibration fits with the concept that the apical turn of the cochlea has amplification and negative feedback (Khanna and Hao, 1998). The observed change in BM amplitude is opposite to that predicted by electromotility; the observed asymmetry of time waveforms in the apical turn is also in the opposite direction from what would be produced by electromotility. In addition, electromotility produces symmetric response at low frequencies, and even if there were nonlinearity in the OHC

motion, the negative feedback would remove it. This suggests that the mechanically induced motility may be controlling the response in the apical turn.

It is harder to deflect the stereocilia in the direction of excitation because the stiffness of the stereocilia is higher in the excitatory direction, as compared to the inhibitory direction, by about a factor of 2 (Strelioff and Flock, 1984). The excitatory to inhibitory ratio at the OHC was between 1.9 and 2.5 (Flock and Strelioff, 1984; Russell et al., 1992). In our experiments at the OHC1, below CF (177 Hz), the ratio of the positive half and the negative half of the velocity magnitude is nearly 2 (Khanna and Hao, 1999b). The observed nonlinearity is consistent with the asymmetry of stereocilia stiffness. Motion of the RL up towards the SV (TM) causes the stereocilia to move in the excitatory direction. The stereocilia stiffness in the excitatory direction is higher. The velocity therefore is reduced. Motion of the RL towards ST causes the stereocilia to move in the inhibitory direction; their stiffness is lower and therefore the velocity is higher. This explanation assumes that the stereocilia stiffness dominates the cochlear micro mechanics near the CF region; therefore, the changes in stiffness are reflected directly in the deflection asymmetry. Support for this concept comes from experiments on lateral line organ in fish (van Netten and Khanna, 1994).

Additional information for the origin of nonlinearity comes from experiments using cisplatin, a drug that is known to produce damage to OHC. The nonlinearity does not change appreciably after the administration of cisplatin even though the function of the OHC is seriously compromised (Jung and Khanna, 1999). If the nonlinear motility of OHC was the source of harmonics, the harmonics should have disappeared.

The slope of the phase curves indicates the time delay associated with the fundamental or harmonic components. The slope of the phase curves is much steeper for the harmonics, indicating that the time delay associated with their generation is larger than that for the fundamental. This would be consistent with the generation of harmonics after the primary event: motion of the RL.

The nonlinear components of the response are very sensitive to trauma. Damage to the cochlea is associated with loss of harmonic amplitude and broadening of harmonic tuning. We are able to predict the outcome of a cochlear mechanics experiment by the shape and sensitivity of the harmonic-tuning curve.

We may ask what the functional significance of the cochlear nonlinearity is. Auditory and speech signals are modulated waves containing both frequency and amplitude modulation of a carrier. The information is contained in the low frequency modulating signals and can be extracted by demodulation. That a demodulation process is present in the peripheral auditory system was demonstrated earlier in cats (Khanna and Teich, 1989a,b). Amplitude and frequency modulated auditory signals were applied to the ear. Strong demodulated signals were found in the single primary auditory nerve fiber response. The response was robust and seen throughout the auditory frequency range and over a wide intensity range.

Demodulation of amplitude modulated waves by the hair cells in the lateral line organ has been shown (van Netten and Khanna, 1993). Similar observations have been made in the fourth and third turns guinea pig temporal bone preparations and in the apical turn of cochlea of living animals (unpublished observations).

An amplitude modulation demodulator consists of a linear amplifier which is followed by a nonlinearity that rectifies the modulated wave (Schwartz, 1990). In the apical turn of the cochlea our evidence supports a linear amplification of the BM vibrations followed by an asymmetrical stereocilia deflection that would demodulate the vibratory signal.

5. Conclusions

The cellular response of the apical turn of the cochlea at the level of RL is nonlinear. When harmonic distortion is used to define nonlinearity, distortion increases with SPL in similar patterns in both the apical and basal turns. When nonlinearity is measured using the fundamental component response, the results are

quite different in the apical and basal turn. The response of the apical turn is quite linear up to high sound pressure levels, while the response in the basal turn is highly nonlinear near CF at low sound pressure levels. Negative feedback in the apical turn linearizes the response at the fundamental frequency. The nonlinear harmonic response originates outside the feedback loop and is therefore not affected by the negative feedback.

Acknowledgements

Research supported by Emil Capita fund. We thank G.T. Kaufman III and P. Andreola for their help in data analysis and preparing the figures.

References

Békésy, G.von., 1960. In: Wever, E.G. (Eds.), Experiments in Hearing. McGraw-Hill, New York.
Bode, H.W., 1945. Network analysis and feedback network design. D. Van Nostrand, New York, NY.
de Boer, E., 1984. Auditory physics. Physical principles in hearing theory II. Phys. Rep. 105, 142–226.
Brownell, W.E., 1983. Observations on a motile response in isolated outer hair cells. In: Webster, W.R., Aitkin, L.M. (Eds.), Mechanisms of Hearing. Monash University press, Clayton, Australia, pp. 5–10.
Brownell, W.E., Bader, C.R., Bertrand, D., de Ribaupierre, Y., 1985. Evoked mechanical responses of isolated hair cells. Science 227, 194–196.
Brundin, L., Flock, Å., Canlon, B., 1989. Sound induced motility of isolated cochlear outer hair cells is frequency selective. Nature 342, 814–816.
Brundin, L., Russell, I.J., 1994. Tuned phasic and tonic motile responses of isolated outer hair cells to direct mechanical stimulation of the cell body. Hear. Res. 73, 35–45.
Cooper, N.P., 1996. Mid-band sensitivity notches in apical cochlear mechanics. In: Lewis, E.R., Long, G.R., Lyon, R.F., Narins, P.M., Steele, C.R., Hecht, P. (Eds.), Diversity in Cochlear Mechanics. World Scientific, Singapore, pp. 298–304.
Cooper, N.P., 1998. Harmonic distortion on the basilar membrane in the basal turn of the guinea-pig cochlea. J. Physiol. 509, 277–288.
Cooper, N.P., Rhode, W.S., 1995. Nonlinear mechanics at the apex of the guinea pig cochlea. Hear. Res. 82, 225–243.
Flock, Å., Strelioff, D., 1984. Graded and nonlinear mechanical properties of sensory hairs in the mammalian hearing organ. Nature 310, 597–599.
Gummer, A.W., Hemmert, W., Zenner, H.P., 1996. Resonant tectorial membrane motion in the inner ear: its crucial role in frequency tuning. Proc. Natl. Acad. Sci. 93, 8727–8732.
Hao, L., Khanna, S.M., 1996. Reissner's membrane vibrations in the apical turn of living guinea pig cochlea. Hear. Res. 99, 176–189.
Hudspeth, A.J., Corey, D.P., 1977. Sensitivity, polarity and conductance change in the response of vertebrate hair cells to controlled mechanical stimuli. Proc. Natl. Acad. Sci. 74 (6), 2407–2411.
ITER, 1989. International team for ear research. Acta Otolaryngol. (Stockh.) (Suppl. 467), 1–279.
Iurato, S., 1961. Submicroscopic structure of the membranous labyrinth: 2. The epithelium of Corti's organ. Z. Zellforsch 53, 259.
Jung H.-W., Khanna, S.M., 1999. Change in the apical turn mechanical response in the guinea pig following Cisplatin. Proceedings of the Symposium on Recent Developments in Auditory Mechanics. Sendai, Japan.
Khanna, S.M., Hao, L.F., 1998. Negative feed back in the apical turn of cochlea. Acoustica. 84 (6), 1175–1176.
Khanna, S.M., Hao, L.F., 1999a. Reticular lamina vibrations in the apical turn of a living guinea pig cochlea. Hear. Res. 132, 15–23.
Khanna, S.M., Hao, L.F., 1999b. Nonlinear vibrations in the apical turn of the cochlea in living guinea pigs. Hear. Res. 135, 89–104.
Khanna, S.M., Koester, C.J., Willemin, J.F., Dandliker, R., Rosskothen., H., 1996. A noninvasive optical system for the study of the function of the inner ear in living animals. In: Tuchin, V. (Ed.), Selected Papers on Coherence Domain Methods in Biomedical Optics. SPIE 2732, 64–81.
Khanna, S.M., Teich, M.C., 1989a. Spectral characteristics of the responses of primary auditory-nerve fibers to amplitude modulated signals. Hear. Res. 39, 143–158.
Khanna, S.M., Teich, M.C., 1989b. Spectral characteristics of the responses of primary auditory-nerve fibers to amplitude modulated signals. Hear. Res. 39, 159–176.
Khanna, S.M., Ulfendahl, M., Flock, Å., 1989a. Dependence of cellular response on signal level. Acta Oto-Laryngol (Stockh.) (Suppl. 467), 195–204.

Khanna, S.M., Ulfendahl, M., Flock, Å., 1989b. Waveforms and spectra of cellular vibrations in the organ of Corti. Acta Oto-Laryngol (Stockh.) (Suppl. 467), 195–204.
Khanna, S.M., Ulfendahl, M., Steele, C.R., 1998. Vibration of reflective beads placed on the basilar membrane. Hear. Res. 116, 71–85.
Koester, C.J., 1980. Scanning mirror microscope with optical sectioning characteristics: applications in ophthalmology. Appl. Opt. 19, 1749–1757.
Koester, C.J., 1990. High efficiency optical sectioning with confocal slits. Trans. Roy. Microsc. Soc. 1, 327–332.
Koester, C.J., Khanna, S.M., Rosskothen, H., Tackaberry, R.B., 1989. Incident light optical sectioning microscope for visualization of cellular structures in the inner ear. Acta Otolaryngol. (Stockh.) (Suppl. 467), 27–34.
Koester, C.J., Khanna, S.M., Rosskothen, H., Tackaberry, R.B., Ulfendahl, M., 1994. Confocal slit divided-aperture microscope: applications in ear research. Appl. Optics 33, 702–708.
Lim, D.J., 1986. Functional structure of the organ of Corti: a review. Hear. Res. 22, 117–146.
Rhode, W.S., 1978. Some observations on cochlear mechanics. J. Acoust. Soc. Am. 64, 158–176.
Robles, L., Ruggero, M.A., Rich, N.C., 1986. Basilar membrane mechanics at the base of the chinchilla cochlea. I. Input output functions, tuning curves, and response phases. J. Acoust. Soc. Am. 80, 1364–1374.
Ruggero, M.A., Rich, N.C., 1991. Application of a commercially manufactured Doppler-shift laser velocimeter to the measurement of basilar-membrane vibration. Hear. Res. 51, 215–230.
Russell, I.J., Kössl, M., Richardson, G.P., 1992. Nonlinear mechanical response of mouse cochlear hair bundles. Proc. R. Soc. Lond. B 250, 217–227.
Sokolich, G.W., 1981. Closed sound delivery system. United States Patent 4251686.
Spoendlin, H., 1972. Innervation densities of the cochlea. Acta Otolaryngol. 73, 235–248.
Steele, C.R., 1974. Behavior of the basilar membrane with pure tone excitation. J. Acoust. Soc. Am. 55, 148–172.
Strelioff, D., Flock, Å., 1984. Stiffness of sensory-cell hair bundles in the isolated guinea pig cochlea. Hear. Res. 15, 19–28.
Schwartz, M., 1990. Information transmission modulation and noise. McGraw-Hill, New York.
Tilney, L.G., Saunders, J.C., 1983. Actin filaments, stereocilia, and hair cells of the bird cochlea. I. Length, number, width and distribution of stereocilia of each hair cell are related to the position of the hair cell on the cochlea. J. Cell Biol. 96, 807–821.
van Netten, S.M., Khanna, S.M., 1993. Mechanical demodulation of hydrodynamic stimuli performed by the lateral line organ. In: Allumn, J.H.J. (Ed.), Progress in Brain Research, vol. 97. Elsevier, Amsterdam, pp. 45–51.
van Netten, S.M., Khanna, S.M., 1994. Stiffness changes of the cupula associated with the mechanics of hair cells in the fish lateral line. Proc. Natl. Acad. Sci. 91, 1549–1553.
Wever, E.G., Lawrence, M., 1954. Physiological Acoustics. Princeton University Press, Princeton, New Jersey.
Willemin, J.F., Dandliker, R., Khanna, S.M., 1988. Heterodyne interferometer for submicroscopic vibration measurements in the inner ear. J. Acoust. Soc. Am. 83, 787–795.
Willemin, J.F., Khanna, S.M., Dandliker, R., 1989. Heterodyne interferometer for cellular vibration measurement. Acta Otolaryngol. (Stockh.) (Suppl. 467), 35–42.
Zwicker, E., 1986. A hardware cochlear nonlinear preprocessing model with active feedback. J. Acoust. Soc. Am. 80, 146–153.
Zwislocki, J., 1948. Theorie der Schneckenmechanik. Qualitative and quantitative analyse. Acta Otolaryngol. (Suppl. 72).